nanomaterials

MDPI

Article

CO_2 Sequestration in the Production of Portland Cement Mortars with Calcium Carbonate Additions

Marius-George Parvan, Georgeta Voicu *, Alina-Ioana Badanoiu, Adrian-Ionut Nicoara and Eugeniu Vasile

Department of Science and Engineering of Oxide Materials and Nanomaterials, Faculty of Applied Chemistry and Material Science, University POLITEHNICA of Bucharest, 1-7 Gh. Polizu Street, District 1, RO-011061 Bucharest, Romania; marius.george.parvan@gmail.com (M.-G.P.); alina.badanoiu@upb.ro (A.-I.B.); adi.nicoara18@gmail.com (A.-I.N.); eugeniu.vasile@upb.ro (E.V.)

* Correspondence: georgeta.voicu@upb.ro

Abstract: The paper presents the obtention and characterization of Portland cement mortars with limestone filler and nano-calcite additions. The nano-calcite was obtained by the injection of CO_2 in a nano-$Ca(OH)_2$ suspension. The resulted nano-$CaCO_3$ presents different morphologies, i.e., polyhedral and needle like crystals, depending on the initial $Ca(OH)_2$ concentration of the suspension. The formation of calcium carbonate in suspensions was confirmed by X-ray diffraction (XRD), complex thermal analysis (DTA-TG), scanning electron microscopy (SEM) and transmission electron microscopy (TEM and HRTEM). This demonstrates the viability of this method to successfully sequestrate CO_2 in cement-based materials. The use of this type of nano-$CaCO_3$ in mortar formulations based on PC does not adversely modify the initial and final setting time of cements; for all studied pastes, the setting time decreases with increase of calcium carbonate content (irrespective of the particle size). Specific hydrated phases formed by Portland cement hydration were observed in all mortars, with limestone filler additions or nano-$CaCO_3$, irrespective of curing time. The hardened mortars with calcium carbonate additions (in adequate amounts) can reach the same mechanical strengths as reference (Portland cement mortar). The addition of nano-$CaCO_3$ in the raw mix increases the mechanical strengths, especially at shorter hardening periods (3 days).

Keywords: Portland cement; nano-$CaCO_3$; limestone filler; carbon footprint reduction; CO_2 sequestration

Citation: Parvan, M.-G.; Voicu, G.; Badanoiu, A.-I.; Nicoara, A.-I.; Vasile, E. CO_2 Sequestration in the Production of Portland Cement Mortars with Calcium Carbonate Additions. *Nanomaterials* **2021**, *11*, 875. https://doi.org/10.3390/nano11040875

Academic Editor: Francesca Romana Lamastra

Received: 9 March 2021
Accepted: 27 March 2021
Published: 30 March 2021

1. Introduction

In recent years there has been a constant interest from political and scientific community in identifying new ways to reduce greenhouse gases to combat global warming and climate change. The cement industry is one of the major contributors to the world's CO_2 emissions; it is generally accepted that the production of one ton of cement (CEM I) can release up to one ton of carbon dioxide [1,2].

Portland cement is obtained by the grounding of clinker with gypsum and other admixtures. The clinker is produced by heating a raw mix, consisting mainly of limestone and clay (marl) up to 1450 °C in a rotary kiln. Several chemical processes take place in the rotary kiln and transform the raw mix in the clinker; limestone calcination is the main chemical process which generates up 60–65% CO_2 of cement manufacturing. CO_2 emissions are also generated by the burning of fuels used to heat the rotary kiln [3].

Portland cement is one of the key ingredients of concrete, which is the third most used substance in the world after air and water [4]. As a result, the reduction in the carbon footprint of cement production has drawn a great deal of attention from scientists around the globe in a unified effort to preserve our planet. One of the currently studied methods for the achievement of a greener cement production is carbon dioxide sequestration in cement-based materials [1–5].

The carbonatation of concrete mixtures produced with various types of cements represent a new approach aiming to sequestrate CO_2 in concrete. Microstructural and

mechanical properties of cement-based materials may be altered by early-age carbonation which often provides hydrates with significant differences [6–19].

A great deal of research has been performed in order to substantiate the use of finely ground limestone (limestone filler -L) as a partial substitute for Portland cement in the attempt to reduce the amount of clinker used in the production of Portland cement and consequently to reduce the green gas emissions associated with this process [20,21]. According to Panesar and Zhang [21], for lower replacement levels (up to 10%) concrete or mortar with limestone filler has similar properties compared with control mix, but the increase of substitution ratio can affect properties such as strength, porosity and permeability. To mitigate these drawbacks research studies were performed using nano-$CaCO_3$ [22–35]. Ge et al. [32] reported that the addition to mortar/concrete of nano-calcium carbonate (in adequate amounts) increases the compressive strength and reduces average pore diameter.

Qin et al. [2] proposed a new technology aiming to reduce the carbon footprint of the cement industry, consisting mainly in the use of the CO_2 generated in cement production to carbonate suspensions of lime with concentrations of 0.17%, 0.34% and 1.02% by mass. The introduction of the resulting nano-calcium carbonate in cement paste improved the mechanical properties and refined the pore structure.

This study assesses the feasibility of producing calcium carbonate suspensions with higher concentrations (0.3% up to 5% nano-$CaCO_3$) by the carbonation of nano-CaO suspensions and to compare their influence on the main properties of Portland cement mortars with the effect determined by limestone filler additions.

2. Materials and Methods

2.1. Materials

The following materials were used in this study:

- calcium oxide nano-powder (<160 nm BET particle size, Sigma Aldrich, Darmstadt, Germany) and CO_2 gas, with 100% concentration;
- Portland cement (PC) CEM I 42.5R, with 3095 cm^2/g Blaine specific surface area and oxide composition presented in Table 1; the PCs oxide composition was assessed by the chemical methods described in European standard EN 196-2:2013 [36];
- limestone filler (L) with 97 wt.% $CaCO_3$ and a fineness corresponding to 5350 cm^2/g Blaine specific surface area.

Table 1. Oxide composition of Portland cement.

Component	CaO	SiO_2	Al_2O_3	Fe_2O_3	MgO	SO_3	LOI
Content (wt.%)	63.78	20.12	4.58	3.99	1.20	2.61	3.72

LOI—loss on ignition.

2.2. Preparation of Cement Pastes and Mortars with Limestone Filler and Nano-$CaCO_3$

$Ca(OH)_2$ aqueous suspension (aq. susp.) in various concentrations (0.5%, 3.7% and 7.4%) were prepared by partially dissolution of nano-CaO in water. The next step consists of CO_2 gas injection in $Ca(OH)_2$ aq. susp., at a rate of 15 dm^3/min. The duration of injection operation was 3 minutes for each liter of $Ca(OH)_2$ aq. susp. In order to produce a homogenous suspension by the reaction of CO_2 with nano-$Ca(OH)_2$, the suspensions were continuously stirred with a magnetic stirrer. The pH of $Ca(OH)_2$ aqueous suspensions (before CO_2 injection) was 12.5 and after the CO_2 injection the pH dropped to 6.5, which suggests the complete carbonation of nano-$Ca(OH)_2$ in the suspension. The density (assessed with a hydrometer) was 1 g/cm^3 for all suspensions. The aqueous suspensions where vigorously stirred and used to produce cement pastes and mortars.

Table 2 shows the composition of the studied cements prepared with limestone filler or carbonated nano-$Ca(OH)_2$ aqueous suspensions.

Table 2. Composition of the studied cements.

Cement	E	L3	L5	L10	L15	CC0.5	CC3.7	CC7.4
Portland cement (wt.%)	100	97	95	90	85	99.65	97.5	95
Limestone filler (wt.%)	0	3	5	10	15	0	0	0
Nano-$CaCO_3$ (wt.%)	0	0	0	0	0	0.35	2.5	5

The amount of nano-$CaCO_3$ was calculated based on the concentration of the aqueous suspensions and the amount of liquid (aq. susp.) used to achieve a liquid to cement ratio of 0.5.

The codification of samples (pastes or mortars) with $Ca(OH)_2$ carbonated aq. susp. was made according to the equivalent dosage of calcium hydroxide, i.e., CC0.5—with 0.5% $Ca(OH)_2$ carbonated aq. susp.; CC3.7—with 3.7% $Ca(OH)_2$ carbonated aq. susp.; CC7.4—with 7.4% $Ca(OH)_2$ carbonated aq. susp.

Mortars were prepared using the cement compositions presented in Table 2, aggregate and water. The cement to aggregate ratio was 0.3 and water to cement ratio = 0.5. The aggregate was CEN standard siliceous sand with the grading fully complying with EN 196-1:2016, Part 1 [37]. The fresh mortars were cast in prism molds (160 × 40 × 40 mm) and compacted by impact. The resulting three mortar specimens (for each composition) were cured in humid environment (R.H. 95%) for 3, 7 and 28 days.

2.3. Methods

The mineralogical composition of materials was assessed by X-ray diffraction (XRD), with a Shimadzu XRD 6000 diffractometer (Shimadzu, Kyoto, Japan), with Ni-filtered CuKα radiation (α = 1.5406 Å), 2θ = 5–65°.

The morphology and microstructure of the materials (nano-$CaCO_3$ and hardened PC mortars with/without limestone or nano-$CaCO_3$ content) were assessed by electron microscopy-scanning electron microscopy (SEM) and transmission electron microscopy (HR-TEM). SEM analysis were performed using a Quanta Inspect F scanning electron microscope (FEI Company, Hillsboro, OR, USA) with a Schottky emission electron beam (1.2 nm resolution at 30 kV and 3 nm at 1 kV for BSE; gold was used for the coating of specimens). The TEM analyses were performed using a TecnaiTM G2 F30 S-TWIN high resolution transmission electron microscope (HR-TEM) (Thermo Fisher—former FEI, Eindhoven, Nederland) equipped with STEM-HAADF detector, EDX and EELS. The average particle size and crystallinity degree were estimated using this method.

The water for standard consistency and setting time of cement pastes was assessed with the methods presented in European standard EN 196—1:2016, Part 3 [38].

Flexural and compressive strength were assessed using a Matest machine ((MATEST, Treviolo, Italy), in accordance with the method presented in European standard EN 196—1:2016, Part 1 [37]; the strength values represent the average of at least three strength values assessed on mortar specimens cured in similar conditions.

3. Results and Discussion

The mineralogical compositions of Portland cement and limestone filler were assessed by XRD. On the XRD pattern of Portland cement (Figure 1a) the following peaks are present: alite (Ca_3SiO_5 or C_3S, JCPDS 31-0301), belite (Ca_2SiO_4 or C_2S, JCPDS 31-0299), tricalcium aluminate ($Ca_3Al_2O_6$ or C_3A, JCPDS 38-1429), and gypsum ($CaSO_4 \cdot 2H_2O$ or $C\bar{S}H_2$, JCPDS 21-0816). For the limestone filler (Figure 1b) the main phase assessed by XRD is calcite ($CaCO_3$, JCPDS 72-1650).

To confirm the presence of calcium carbonate in aq. susps., 1 ml from each suspension (vigorously stirred in order to be homogenous) was sampled and dried at 50 °C up to constant weight. The XRD patterns of the resulting powders (Figure 2) showed the presence of a single crystalline compound—$CaCO_3$ (JCPDS 83-1762).

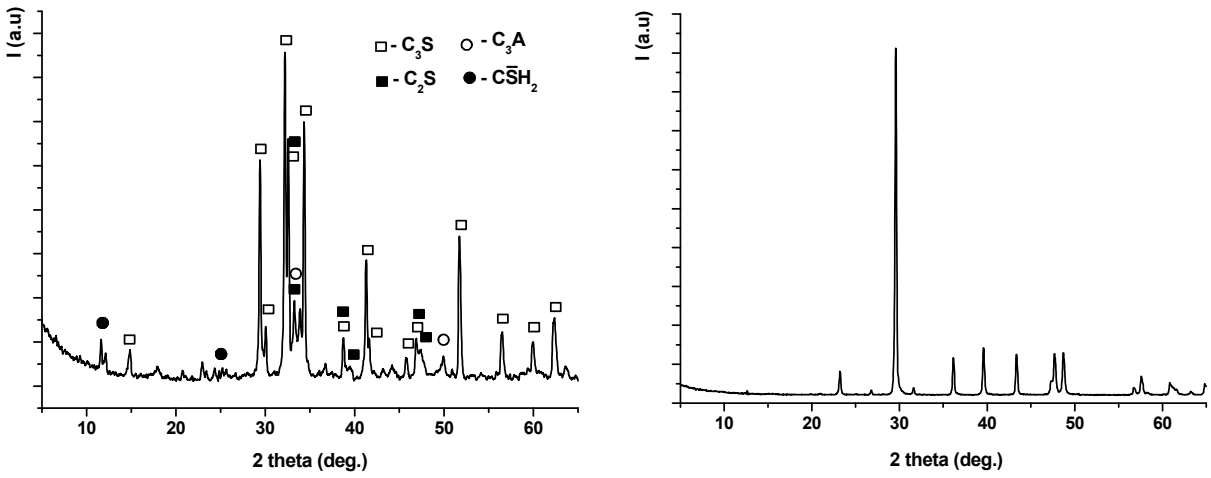

(**a**) (**b**)

Figure 1. X-ray diffraction pattern of Portland cement (**a**), and of limestone filler (**b**).

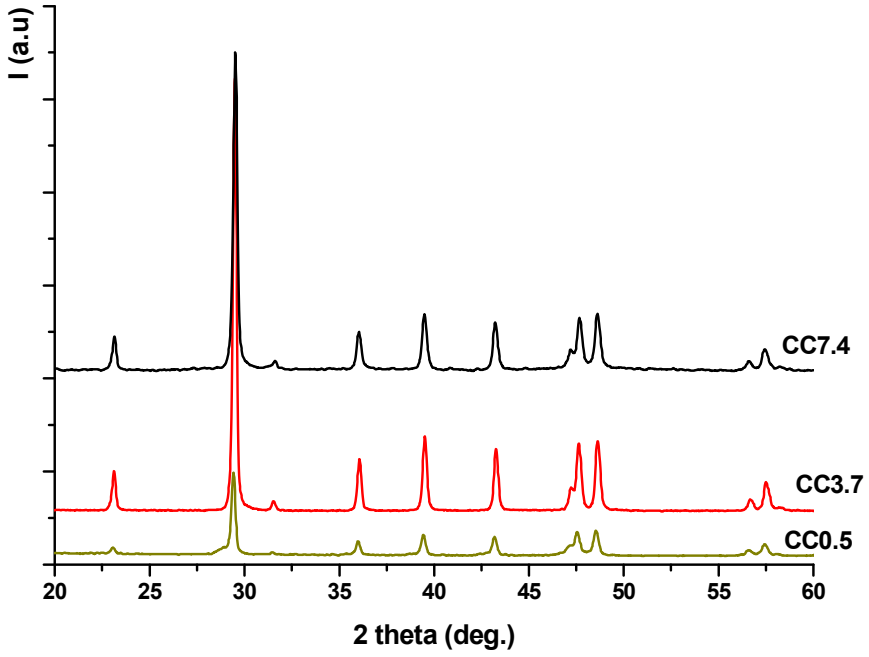

Figure 2. X-ray diffraction patterns of dried powders.

The differential thermal analysis (DTA) curves of dried powders (Figure 3) show an intense endothermic effect with maximum at 748–773 °C, with a corresponding weight loss assessed on TG curves between 650–800 °C; this effect is attributed to the $CaCO_3$ decarbonation [39] and is in good correlation with the results obtained by XRD analysis, previously presented. Because decarbonation process occurs below 800 °C, it is suggested that carbonate phases are microcrystalline [39].

As presented in Figure 4, calcium carbonate powders have different morphologies which can be correlated with their concentration in aq. susp. One can observe the presence of $CaCO_3$ polyhedral crystals in the SEM images (Figure 4a–d) of the powders as a result of the drying of carbonated aq. susp. with 0.5% and 3.7% $Ca(OH)_2$; these crystals are the result of the $Ca(OH)_2$ carbonation. The size of $CaCO_3$ crystals increases with the increase of the initial concentration of $Ca(OH)_2$ aq. susp; for an initial concentration of 7.4% $Ca(OH)_2$ in aq. susp. the resulted $CaCO_3$ crystals have elongated shapes and forms flower-like

aggregates (Figure 4e,f). These shapes (polyhedral or elongated) of $CaCO_3$ crystals were also assessed in other studies [40–42]. These results are in good correlation with those obtained by XRD and DTA-TG analyses.

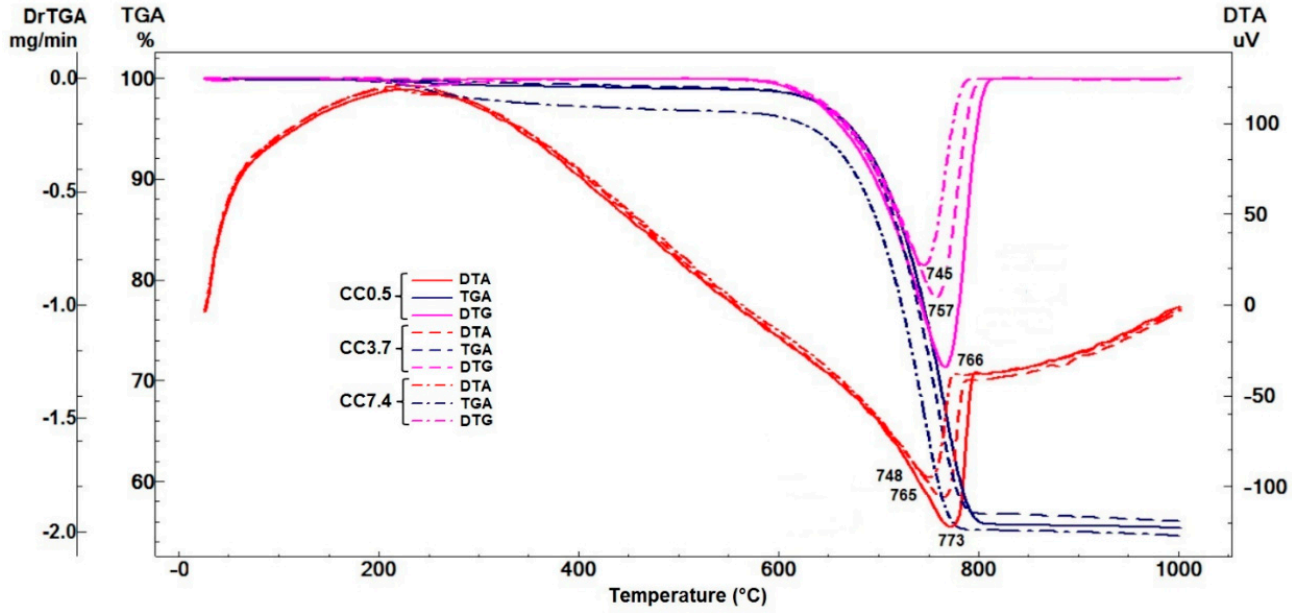

Figure 3. Thermal analysis of dried powders CC0.5, CC3.7 and CC7.4.

The morphology of calcium carbonate crystals was also assessed by high resolution transmission electron microscopy (HR-TEM), as shown in Figure 5. This method permits an assessment of the total conversion of $Ca(OH)_2$ nano-grains in calcium carbonate, irrespective of the initial concentration in nano-CaO of the starting suspension (Figure 5b,d,f); the size of crystals assessed by HR-TEM starts in tens of nanometers (for CC0.5—Figure 5a) and increases with the initial concentration of $Ca(OH)_2$ aq. susp., reaching hundreds of nanometers for CC3.4 and CC7.4 (Figure 5c,e).

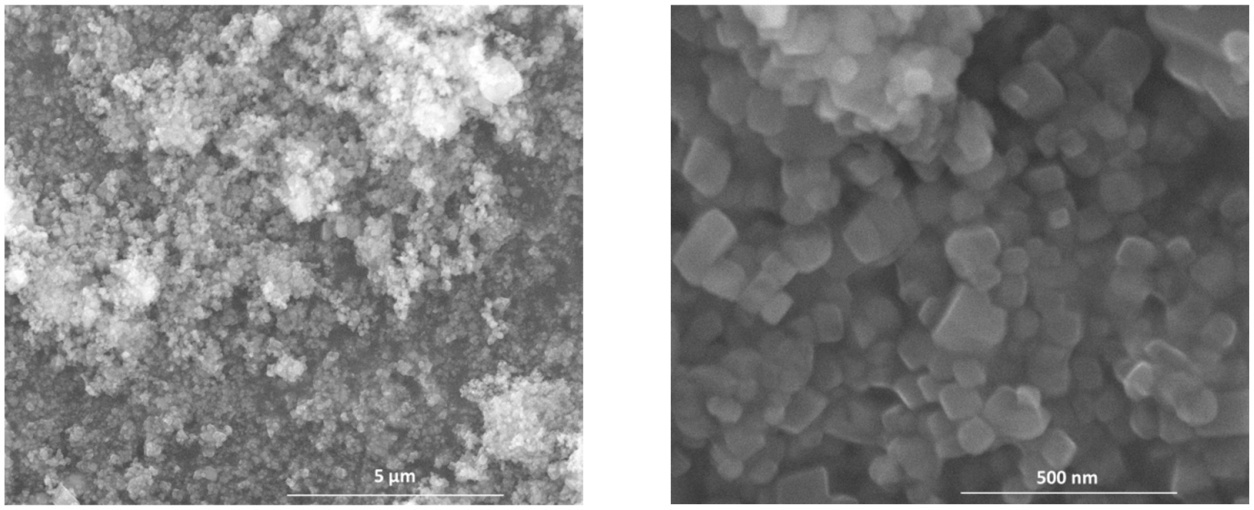

(**a**) (**b**)

Figure 4. *Cont.*

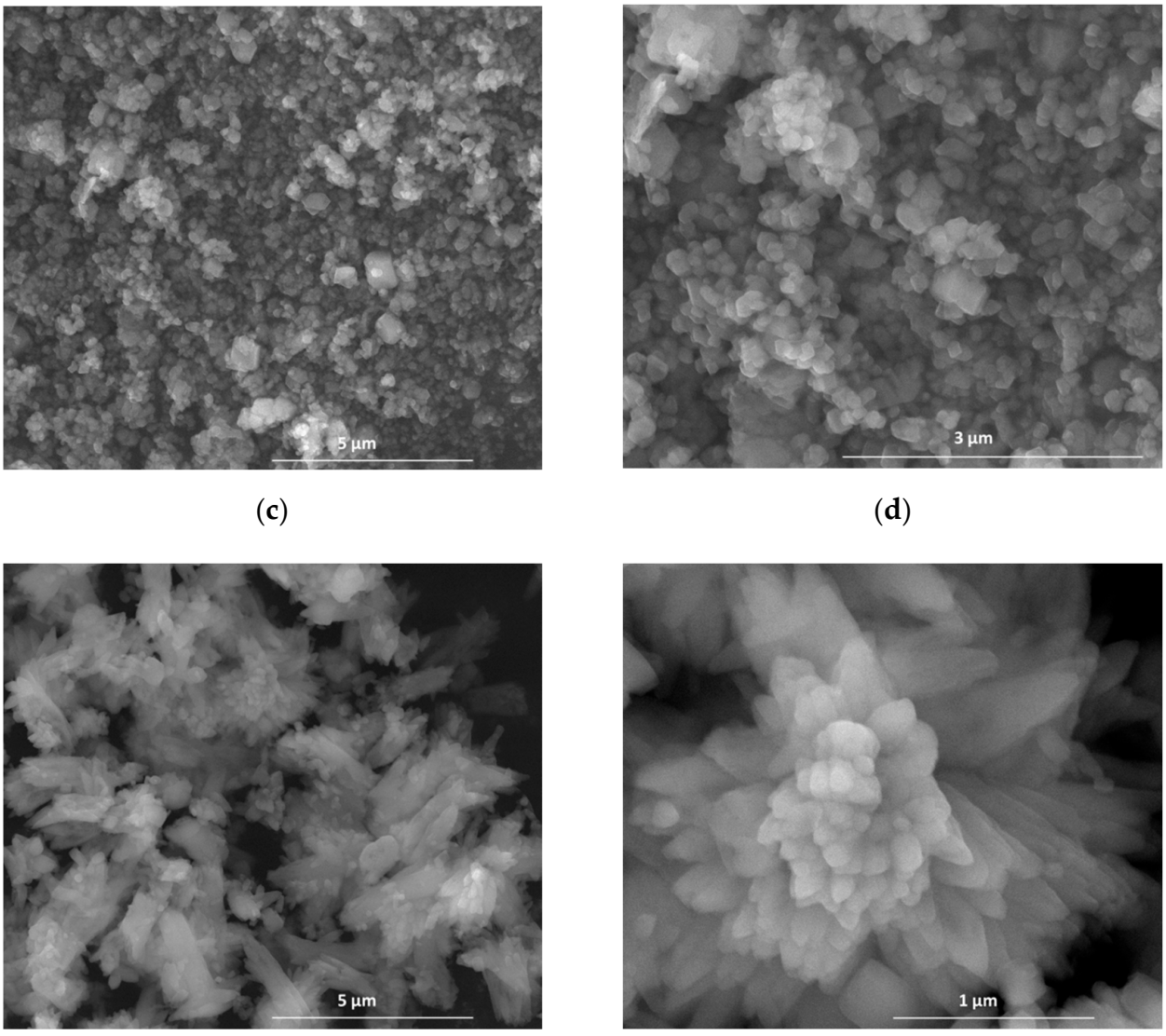

Figure 4. Scanning electron microscopy (SEM) images of dried powders CC0.5 (**a**,**b**), CC3.7 (**c**,**d**) and CC7.4 (**e**,**f**).

The values of water for standard consistency of pastes decrease (with respect to reference—PC paste) with the increase of limestone filler (L) content (Figure 6a). Yahia et al. [43] noticed a similar behaviour for Portland cements with limestone filler additions, i.e., for a given water to cement ratio, there is an optimum value of powder content that can ensure suitable fresh properties of the mixture. These authors explain this by a physical effect determined by limestone filler particles which are smaller compared with those of Portland cement and fill the voids existent between them; this reduces the interparticle friction and liberates part of the mixing water otherwise entrapped in the system, thus increasing the fluidity of the fresh paste. For the specimens with nano-$CaCO_3$, one can also notice the decrease of water for standard consistency with the increase in the nano-$CaCO_3$ amount (with reference to PC paste), but the values of water for standard consistency are higher compared with those assessed for cement with limestone content (see, for example, the cements with 5% limestone filler L5 and 5% nano $CaCO_3$ CC7.4). This is in good agreement with the previously mentioned explanation, given the much smaller dimensions of this type of calcium carbonate compared with the limestone particles.

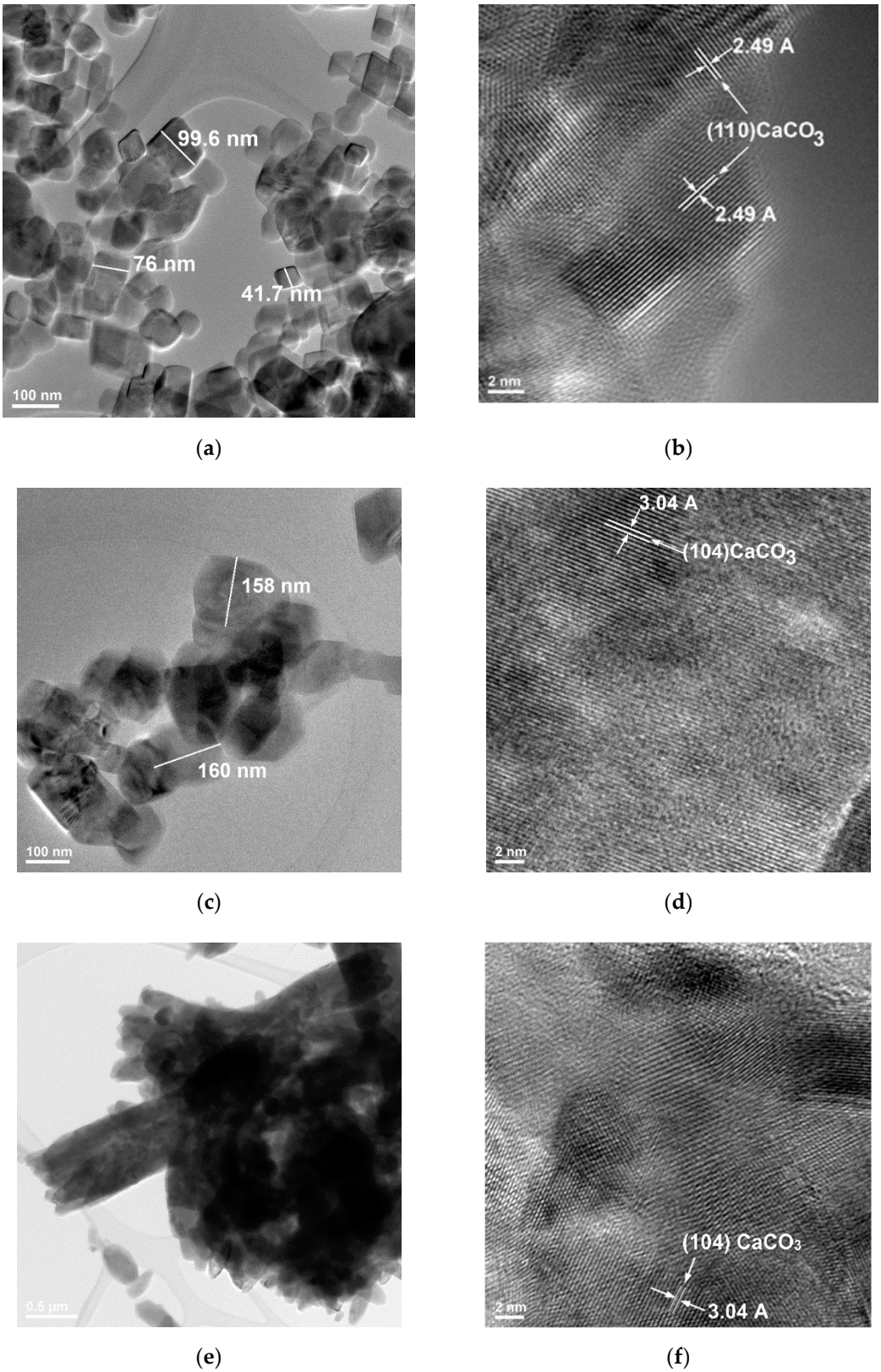

Figure 5. Transmission electron microscopy (TEM) (**a**,**c**,**e**) and HRTM (**b**,**d**,**f**) images of dried powders CC0.5 (**a**,**b**), CC3.7 (**c**,**d**) and CC7.4 (**e**,**f**).

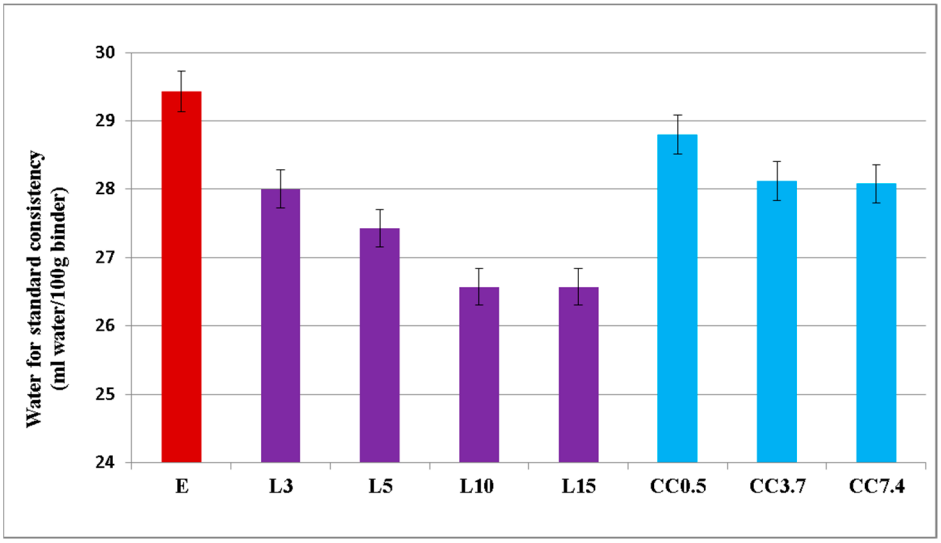

(**a**)

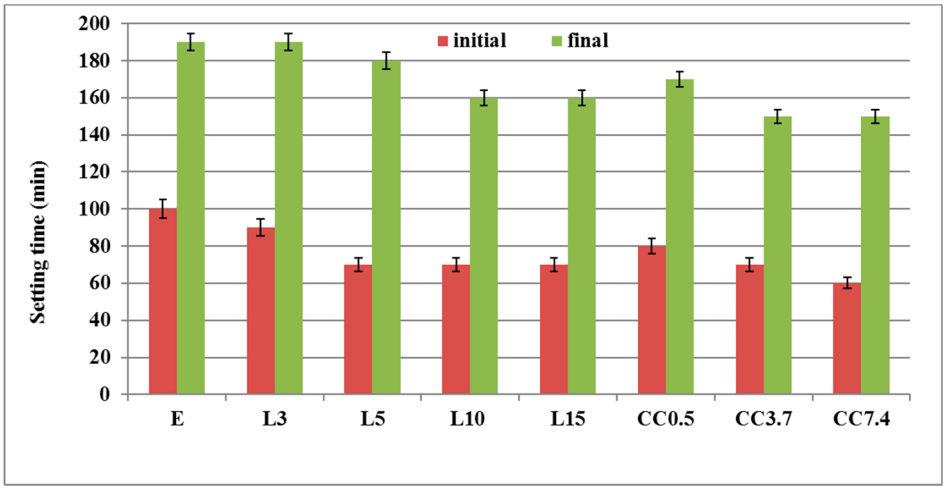

(**b**)

Figure 6. Water for standard consistency (**a**) and setting time (**b**) of binding pastes.

For all studied pastes, the setting time decreases with the increase of calcium carbonate content (Figure 6b); the $CaCO_3$ particles act as crystallization sites for the newly formed hydrates (in the reaction of PC with water). The smaller values for final setting time assessed for the composition with nano-carbonate (see for example CC7.4 compared with L5) can be also due to the high fineness of calcium carbonate (nano powder).

The evolution of mechanical strengths was assessed on mortars hardened for 3, 7 and 28 days—Figure 7. As expected, both compressive and flexural strengths increase with the increase in curing time from 3 to 28 days, due to the development of PC hydration and the hardening process. The substitution of PC with 3% and 5% limestone filler does not substantially modify the mechanical strengths with reference to E (PC), but the increase in substitution rate has a negative influence especially after 28 days of hardening. This is explained by the dilution effect of cement—limestone filler substitutes for the PC which is the active component of the binder (see Table 2).

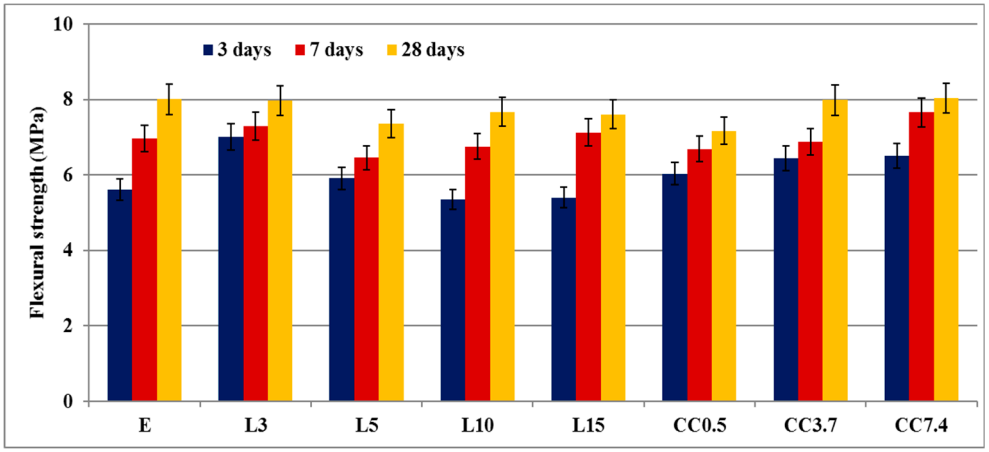

(**a**)

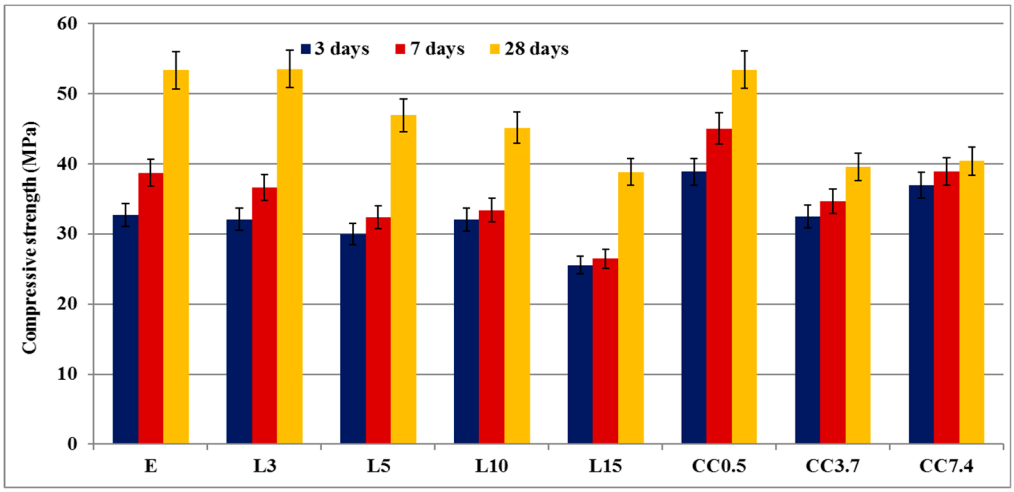

(**b**)

Figure 7. Mechanical strengths of mortars versus hardening time: flexural strength (**a**) and compressive strength (**b**).

The addition of nano-$CaCO_3$ in the raw mix, increases the mechanical strength of the mortars, especially at shorter periods of time (3 and 7 days). The important increase of compressive strengths assessed for CC0.5 (with reference to E) can be explained by an adequate microstructure (refined pore structure) in which a higher amount of hydrates are formed (due to the nucleation effect determined by the $CaCO_3$ nanoparticles) which results in the reduction of the porosity.

Figure 8 shows the SEM images of mortars cured for 28 days. The main phases assessed by this method are: hexagonal plate-like crystals attributed to $Ca(OH)_2$ (CH), fine needles and films attributed to calcium silicate hydrates (CSH), well defined needle-shaped formations characteristic of ettringite (AFt), monoclinic gypsum (G) crystals, parallel plates forming a beam characteristic of the calcium mono-sulfate aluminate hydrate (AFm) phase and polyhedral particles of calcium carbonate (CC).

This method does not permit the assessment of any new hydration products when the calcium carbonate additions (with different grain sizes) are used as additions to Portland cement.

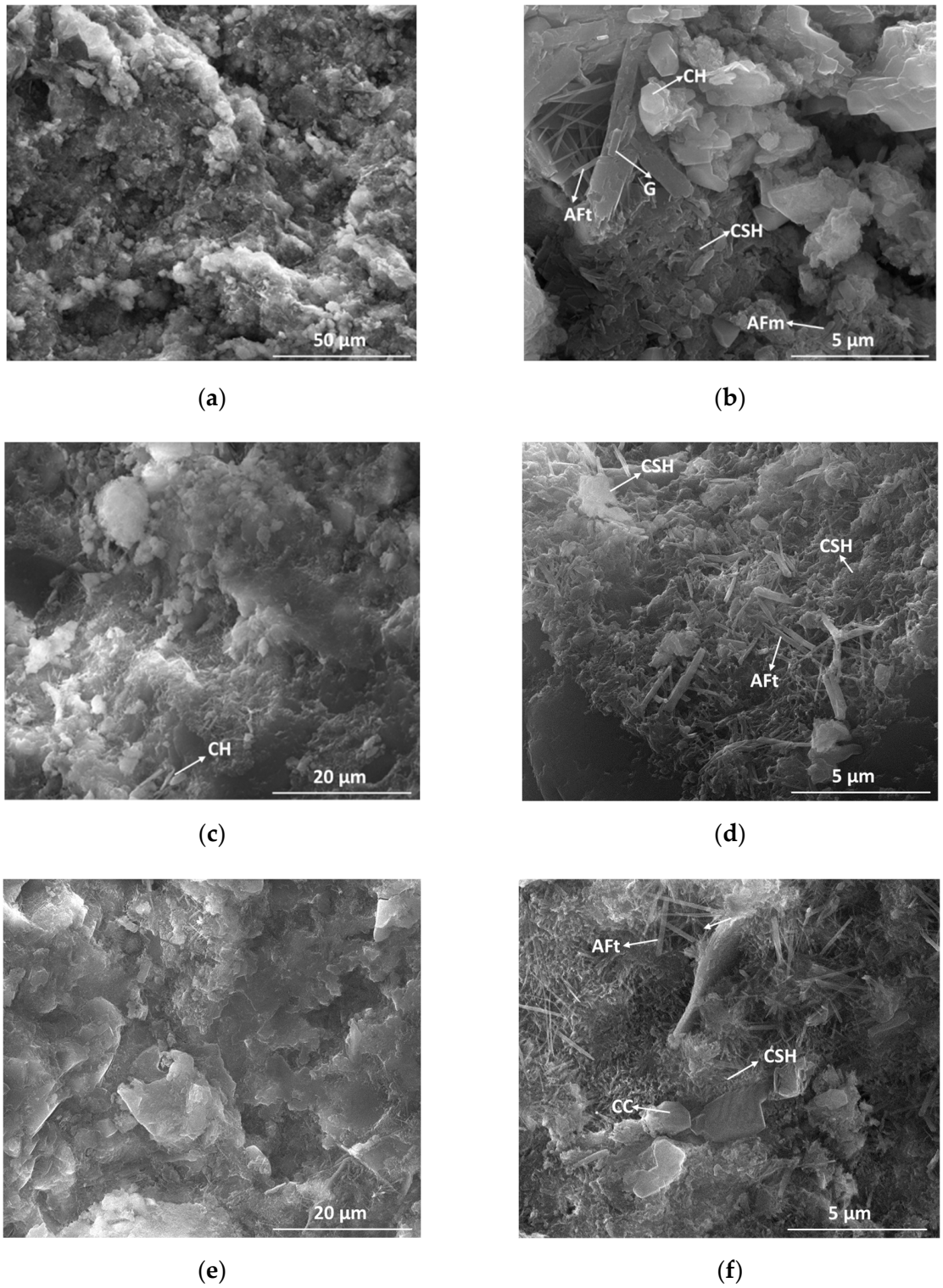

Figure 8. *Cont.*

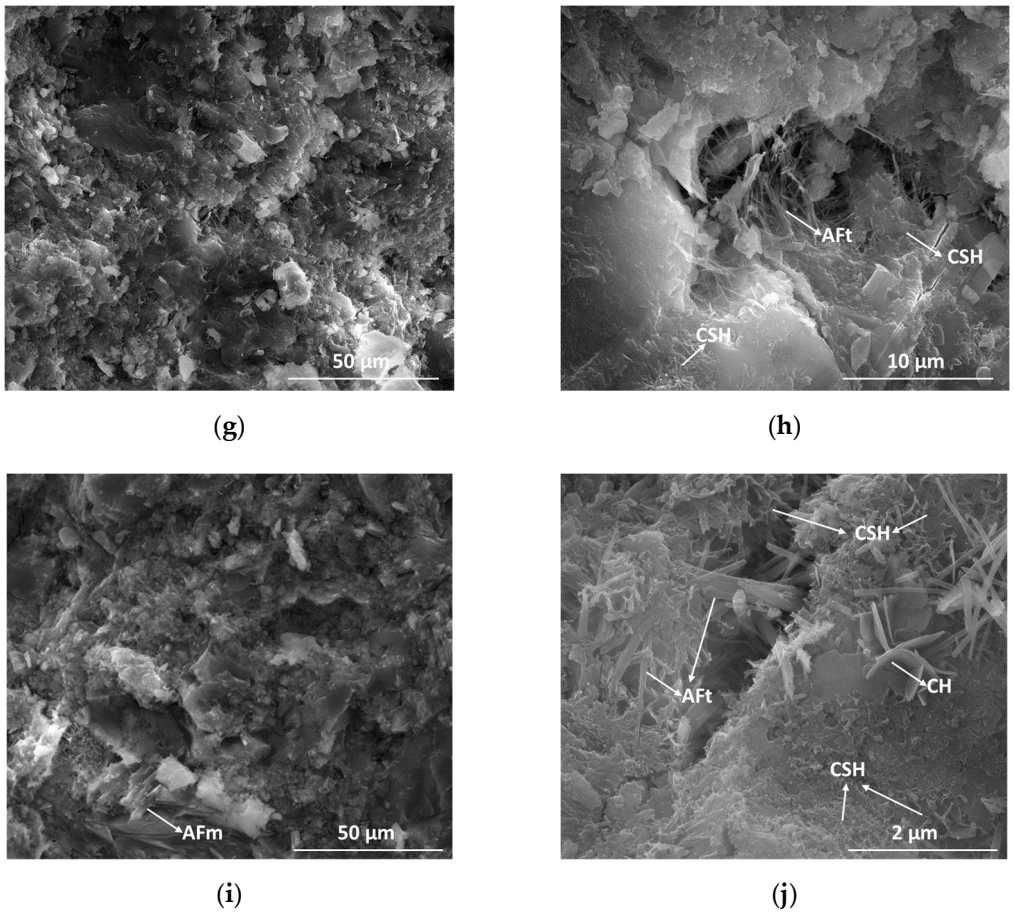

Figure 8. SEM images of hardened mortars at 28 days: E (**a**,**b**), L3 (**c**,**d**), L15 (**e**,**f**), CC0.5 (**g**,**h**) and CC7.4 (**i**,**j**).

4. Conclusions

The experimental results presented in this study demonstrate that carbon dioxide can be successfully sequestered in cement-based materials.

CO_2 sequestration in nano-$CaCO_3$ was obtained by the injection of CO_2 in a nano-$Ca(OH)_2$ suspension. The resulting nano-$CaCO_3$ particles present different morphologies, i.e., polyhedral and needle like crystals, depending on the initial $Ca(OH)_2$ concentration of the suspension.

The use of this type of nano-$CaCO_3$ in Portland cement pastes determines a decrease in the water for standard consistency with reference to PC paste, but the values of water for standard consistency are higher as compared with those assessed for the cement with limestone filler (in the same amount); this is due to the much smaller dimensions of this nano-calcium carbonate compared with the limestone particles.

The use of this nano-carbonate does not adversely modify the initial and final setting time of cements; for all studied pastes, the setting time decreases with the increase of calcium carbonate content (irrespective of the particle size).

Specific hydrated phases formed by Portland cement hydration were observed in all mortars, with limestone filler additions or nano-$CaCO_3$, irrespective of curing time.

The hardened mortars with calcium carbonate additions (in adequate amounts) can reach the same mechanical strengths as reference (Portland cement mortar). The addition of nano-$CaCO_3$ in the raw mix increases the mechanical strengths, especially at shorter hardening periods (3 days).

Author Contributions: Conceptualization, G.V.; investigation, M.-G.P., G.V.; A.-I.N., A.-I.B., E.V.; data curation, G.V.; writing—original draft preparation, M.-G.P., G.V.; writing—review and editing, M.-G.P., G.V.; A.-I.N., A.-I.B., E.V.; supervision, G.V. and A.-I.B.; All authors have read and agreed to the published version of the manuscript.

Funding: This research received no external funding.

Data Availability Statement: Not applicable.

Acknowledgments: The work has been funded by the Operational Programme Human Capital of the Ministry of European Funds through the Financial Agreement 51668/09.07.2019, SMIS code 124705. The SEM analyses obtained on the samples were possible due to EU-funding project POSCCE-A2-O2.2.1-2013-1/Priority Axe 2, Project No. 638/12.03.2014, ID 1970, SMIS-CSNR code 48652.

Conflicts of Interest: The authors declare no conflict of interest. The funders had no role in the design of the study; in the collection, analyses, or interpretation of data; in the writing of the manuscript, or in the decision to publish the results.

References

1. Kaliyavaradhan, S.K.; Ling, T.C.; Mo, K.H. CO_2 sequestration of fresh concrete slurry waste: Optimization of CO_2 uptake and feasible use as a potential cement binder. *J. CO_2 Util.* **2020**, *42*, 101330. [CrossRef]
2. Qin, L.; Gao, X.; Li, Q. Upcycling carbon dioxide to improve mechanical strength of Portland cement. *J. Clean. Prod.* **2018**, *196*, 726–738. [CrossRef]
3. CEMBUREAU (The European Cement Association). Our 2050 Roadmap: The 5C Approach, Clinker. Available online: https://lowcarboneconomy.cembureau.eu/carbon-neutrality/our-2050-roadmap-the-5c-approach-clinker/ (accessed on 6 January 2020).
4. CEMBUREAU (The European Cement Association). The Role of Cement in the 2050 Low Carbon Economy. Available online: https://cembureau.eu/media/cpvoin5t/cembureau_2050roadmap_lowcarboneconomy_2013-09-01.pdf (accessed on 6 January 2020).
5. Youn, M.H.; Park, K.T.; Lee, Y.H.; Kang, S.P.; Lee, S.M.; Kim, S.S.; Kim, Y.E.; Ko, Y.N.; Jeong, S.K.; Lee, W. Carbon dioxide sequestration process for the cement industry. *J. CO_2 Util.* **2019**, *34*, 325–334. [CrossRef]
6. Monkman, S.; MacDonald, M. On carbon dioxide utilization as a means to improve the sustainability of ready-mixed concrete. *J. Clean. Prod.* **2017**, *167*, 365–375. [CrossRef]
7. Li, X.; Ling, T.C. Instant CO_2 curing for dry-mix pressed cement pastes: Consideration of CO_2 concentrations coupled with further water curing. *J. CO_2 Util.* **2020**, *38*, 348–354. [CrossRef]
8. Mo, L.; Zhang, F.; Deng, M. Mechanical performance and microstructure of the calcium carbonate binders produced by carbonating steel slag paste under CO_2 curing. *Cem. Concr. Res.* **2016**, 88217–88226. [CrossRef]
9. Rodríguez de Sensale, G.; Rodríguez Viacava, I. A study on blended Portland cements containing residual rice husk ash and limestone filler. *Constr. Build. Mater.* **2018**, *166*, 873–888. [CrossRef]
10. Celik, K.; Hay, R.; Hargis, C.W.; Moon, J. Effect of volcanic ash pozzolan or limestone replacement on hydration of Portland cement. *Constr. Build. Mater.* **2019**, *197*, 803–812. [CrossRef]
11. Celik, K.; Meral, C.; Petek Gursel, A.; Mehta, P.K.; Horvath, A.; Monteiro, P.J.M. Mechanical properties, durability, and life-cycle assessment of self-consolidating concrete mixtures made with blended Portland cements containing fly ash and limestone powder. *Cem. Concr. Compos.* **2015**, *56*, 59–72. [CrossRef]
12. Celik, K.; Meral, C.; Mancio, M.; Mehta, P.K.; Monteiro, P.J.M. A comparative study of self-consolidating concretes incorporating high-volume natural pozzolan or high-volume fly ash. *Constr. Build. Mater.* **2014**, *67*, 14–19. [CrossRef]
13. Rostami, V.; Shao, Y.; Boyd, A.J.; He, Z. Microstructure of cement paste subject to early carbonation curing. *Cem. Concr. Res.* **2012**, *42*, 186–193. [CrossRef]
14. Zhang, D.; Ghouleh, Z.; Shao, Y. Review on carbonation curing of cement-based materials. *J. CO_2 Util.* **2017**, *21*, 119–131. [CrossRef]
15. Kupwade-Patil, K.; Al-Aibani, A.F.; Abdulsalam, M.F.; Mao, C.; Bumajdad, A.; Palkovic, S.D.; Büyüköztürk, O. Microstructure of cement paste with natural pozzolanic volcanic ash and Portland cement at different stages of curing. *Constr. Build. Mater.* **2016**, *113*, 423–441. [CrossRef]
16. Celik, K.; Jackson, M.D.; Mancio, M.; Meral, C.; Emwas, A.H.; Mehta, P.K.; Monteiro, P.J.M. High-volume natural volcanic pozzolan and limestone powder as partial replacements for Portland cement in self-compacting and sustainable concrete. *Cem. Concr. Compos.* **2014**, *45*, 136–147. [CrossRef]
17. Mo, L.; Panesar, D.K. Accelerated carbonation—A potential approach to sequester CO_2 in cement paste containing slag and reactive MgO. *Cem. Concr. Compos.* **2013**, *43*, 69–77. [CrossRef]
18. Hay, R. *Development, Durability Studies and Application of High Performance Green Hybrid Fiber-Reinforced Concrete (HP-G-HyFRC) for Sustainable Infrastructure and Energy Efficient Buildings*; Engineering—Civil and Environmental Engineering, University of California Berkeley: Berkeley, CA, USA, 2015.

19. Jang, J.G.; Lee, H.K. Microstructural densification and CO_2 uptake promoted by the carbonation curing of belite-rich Portland cement. *Cem. Concr. Res.* **2016**, *82*, 50–57. [CrossRef]
20. Gupta, S.; Mohapatra, B.N.; Bansal, M. A review on development of Portland limestone cement: A step towards low carbon economy for Indian cement industry. *Curr. Res. Green Sustain. Chem.* **2020**, *3*, 100019. [CrossRef]
21. Panesar, D.K.; Zhang, R. Performance comparison of cement replacing materials in concrete: Limestone fillers and supplementary cementing materials—A review. *Constr. Build. Mater.* **2020**, *25*, 1118866. [CrossRef]
22. Ashraf, W. Carbonation of cement-based materials: Challenges and opportunities. *Constr. Build. Mater.* **2016**, *120*, 558–570. [CrossRef]
23. Ahmad, S.; Assaggaf, R.A.; Maslehuddin, M.; Al-Amoudi, O.S.B.; Adekunle, S.K.; Ali, S.I. Effects of carbonation pressure and duration on strength evolution of concrete subjected to accelerated carbonation curing. *Constr. Build. Mater.* **2017**, *136*, 565–573. [CrossRef]
24. Carvalho, S.Z.; Vernilli, F.; Almeida, B.; Oliveira, M.D.; Silva, S.N. Reducing environmental impacts: The use of basic oxygen furnace slag in Portland cement. *J. Clean. Prod.* **2018**, *172*, 385–390. [CrossRef]
25. Lu, B.; Shi, C.; Zhang, J.; Wang, J. Effects of carbonated hardened cement paste powder on hydration and microstructure of Portland cement. *Constr. Build. Mater.* **2018**, *186*, 699–708. [CrossRef]
26. El-Hassan, H.; Shao, Y. Early carbonation curing of concrete masonry units with Portland limestone cement. *Cem. Concr. Compos.* **2015**, *62*, 168–177. [CrossRef]
27. Park, S. Simulating the carbonation of calcium sulfoaluminate cement blended with supplementary cementitious materials. *J. CO_2 Util.* **2020**, *41*, 101286. [CrossRef]
28. Zajac, M.; Lechevallier, A.; Durdzinski, P.; Bullerjahn, F.; Skibsted, J.; Haha, M.B. CO_2 mineralisation of Portland cement: Towards understanding the mechanisms of enforced carbonation. *J. CO_2 Util.* **2020**, *38*, 398–415. [CrossRef]
29. Chen, T.; Gao, X. Effect of carbonation curing regime on strength and microstructure of Portland cement paste. *J. CO_2 Util.* **2019**, *34*, 74–86. [CrossRef]
30. Ho, L.S.; Nakarai, K.; Ogawa, Y.; Sasaki, T.; Morioka, M. Effect of internal water content on carbonation progress in cement-treated sand and effect of carbonation on compressive strength. *Cem. Concr. Compos.* **2018**, *85*, 9–21. [CrossRef]
31. Mehta, K.P.; Monteiro, P.J.M. *Concrete: Microstructure, Properties, and Materials*, 3rd ed.; McGraw-Hill Publishing: New York, NY, USA, 2006. [CrossRef]
32. Ge, Z.; Wang, K.; Sun, R.; Huang, D.; Hu, Y. Properties of self-consolidating concrete containing nano-$CaCO_3$. *J. Sustain. Cem. Mater.* **2014**, 191–200. [CrossRef]
33. Qian, X.; Wang, J.; Wang, L.; Fang, Y. Enhancing the performance of metakaolin blended cement mortar through in-situ production of nano to sub-micro calcium carbonate particles. *Constr. Build. Mater.* **2019**, *196*, 681–691. [CrossRef]
34. Hosan, A.; Shaikh, F.U.A. Influence of nano-$CaCO_3$ addition on the compressive strength and microstructure of high volume slag and high volume slag-fly ash blended pastes. *J. Build. Eng.* **2020**, *27*. [CrossRef]
35. Cosentino, I.; Liendo, F.; Arduino, M.; Restuccia, L.; Bensaid, S.; Deorsola, F.; Ferro, G.A. Nano $CaCO_3$ particles in cement mortars towards developing a circular economy in the cement industry. *Procedia Struct. Integr.* **2020**, *26*, 155–165. [CrossRef]
36. EN 196–2. Part 2. Testing Methods for Cements—Part 2: Chemical Analysis of Cement. 2013.
37. EN 196–1. Part 1. Methods of Testing Cement—Part 1: Determination of Strength. 2006.
38. EN 196–1. Part 3. Methods of Testing Cement—Part 3: Determination of Setting Time and Soundness. 2016.
39. Badanoiu, A.; Paceagiu, J.; Voicu, G. Hydration and hardening processes of Portland cements obtained from clinkers mineralized with fluoride and oxides. *J. Therm. Anal. Calor.* **2011**, *103*, 879–888. [CrossRef]
40. Li, Z.; Xing, L.; Xiang, J.; Liang, X.; Zhao, C.; Sai, H.; Li, F. Morphology controlling of calcium carbonate by self-assembled surfactant micelles on PET substrate. *RSC Adv.* **2014**, 31210–31218. [CrossRef]
41. Chen, J.; Jiang, M.; Su, M.; Han, J.; Li, S.; Wu, Q. Mineralization of calcium carbonate induced by egg substrate and an electric field. *Chem. Eng. Technol.* **2019**, *42*, 1525–1532. [CrossRef]
42. Chen, Q.; Ding, W.; Peng, T.; Sun, H. Synthesis and characterization of calcium carbonate whisker from yellow phosphorus slag. *Open Chem.* **2020**, *18*, 347–356. [CrossRef]
43. Yahia, A.; Tanimura, M.; Shimoyama, Y. Rheological properties of highly flowable mortar containing limestone filler-effect of powder content and W/C ratio. *Cem. Concr. Res.* **2005**, *35*, 532–539. [CrossRef]